Experimental and Solid-State Computational Study of Structural and Dynamic Properties in the Equilibrium Form of Temazepam

ARTICLE *in* THE JOURNAL OF PHYSICAL CHEMISTRY B · MAY 2014

Impact Factor: 3.3 · DOI: 10.1021/jp502609b · Source: PubMed

8 AUTHORS, INCLUDING:

Aleksandra Pajzderska
Adam Mickiewicz University
45 PUBLICATIONS **141** CITATIONS
SEE PROFILE

Marcin Jarek
Adam Mickiewicz University
15 PUBLICATIONS **37** CITATIONS
SEE PROFILE

Jadwiga Mielcarek
Poznan University of Medical Sciences
57 PUBLICATIONS **275** CITATIONS
SEE PROFILE

THE JOURNAL OF PHYSICAL CHEMISTRY B

Article

pubs.acs.org/JPCB

Experimental and Solid-State Computational Study of Structural and Dynamic Properties in the Equilibrium Form of Temazepam

Aleksandra Pajzderska,*[,†] Kacper Drużbicki,[‡,§] Miguel A. Gonzalez,[∥] Jacek Jenczyk,[⊥] Barbara Peplińska,[⊥,#] Marcin Jarek,[⊥] Jadwiga Mielcarek,[⊗] and Jan Wąsicki[†]

[†]Faculty of Physics, A. Mickiewicz University, ul. Umultowska 85, 61-614 Poznań, Poland

[‡]Department of Chemical Physics, Faculty of Chemistry, Jagiellonian University, Ingardena Street 3, 30-060 Cracow, Poland

[§]Frank Laboratory of Neutron Physics, Joint Institute for Nuclear Research, 141980, Dubna, Russia

[∥]Institute Laue Langevin, B.P. 156x, 38042 Grenoble Cedex 9, France

[⊥]The NanoBioMedical Center, A. Mickiewicz Univeristy, Umultowska Street, Poznań, Poland

[#]Department of Macromolecular Physics, Faculty of Physics, A. Mickiewicz University, ul. Umultowska 85, 61-614 Poznań, Poland

[⊗]Department of Inorganic and Analytical Chemistry, Poznań University of Medical Sciences, Grunwaldzka 6, 60-780 Poznań, Poland

ABSTRACT: Structural properties and rotational dynamics of methyl groups in the most stable form of temazepam were investigated by means of ^{13}C CP MAS NMR, quasielastic neutron scattering (QENS), and ^{1}H NMR spin−lattice relaxation methods. The QENS and ^{1}H NMR studies reveal the inequivalency of methyl groups, delivering their activation parameters. The structural properties of the system were explored in frame of periodic density functional theory (DFT) computations, giving insight into the reorientational barriers and providing understanding of the solid-state NMR results. The theoretical computations are shedding light on the intermolecular interactions along their relation with particular asymmetric structural units.

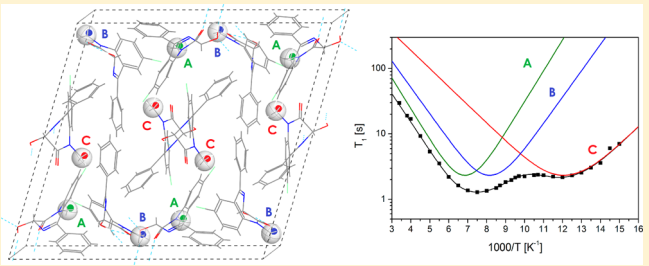

I. INTRODUCTION

Temazepam [7-chloro-3-hydroxy-1-methyl-5-phenyl-1,3-dihydro-2H-1,4-benzodiazepin-2-one, $C_{16}H_{13}ClN_2O_2$] belongs to a group of benzodiazepine derivatives, the most numerous and continuously developed group of anxiolytic drugs, showing strong antianxiety, sedative, sleep inducing, myorelaxing, and anticonvulsive effects.[1,2] Only the compounds with a nitric group or halogen at position C_7 of the benzodiazepine ring are pharmacologically active. Of great significance is the presence of the phenyl ring at position C_5 as the compounds with other substituents at this position are not pharmacologically active. The presence of a methyl group at position 1 enhances the therapeutic effect and facilitates resorption, while the hydroxyl group shortens the time of activity and increases metabolism.[3]

The mechanism of drug activity is strictly related to its molecular structure which determines the possibility of attachment of a therapeutic substance to a specific receptor to produce a desired biological effect. Prediction and analysis of interactions between drugs and receptors needs the information on the conformational space of drugs. Moreover, it is recognized that atomic and molecular motions may influence the efficiency of the quoted binding as well as affect the specific receptor. Hence the dynamic aspect of molecular systems is interesting from the point of view of pharmaceutical science. Yet the understanding of microscopic details of molecular motions along with their relationship to the structural properties remain very limited. More results from multiple systems need to be gathered to create a coherent global picture of the influence of molecular flexibility and dynamics on the bioactivity. The advantage of studying molecular drugs in the well-defined crystal environment has an advantage of being free of the solute effects and the cellular environment. Even in the case of temazepam, multiple possible polymorphic forms exist, which are driven by specific interactions and molecular dynamics. The molecular dynamics is also interesting, since it may promote the solubility of a given polymorph and hence influence the bioavailability.

Despite the wide pharmacological and pharmaceutical literature on the temazepam, there are no systematic studies of its physicochemical properties. The patent literature[4−6] gives information concerning the melting point of different polymorphs of temazepam as well as infrared (IR) absorption and powder X-ray diffraction (PXRD) data, which are used to identify the polymorph. For the first time the structure of temazepam (form 0, anhydrous) was determined in ref 7, and very recently the authors[8] solved the crystallographic structure of the two anhydrous forms of temazepam (named forms X and forms VI).

Received: March 15, 2014
Revised: May 30, 2014

   dx.doi.org/10.1021/jp502609b | J. Phys. Chem. B XXXX, XXX, XXX−XXX

In this paper we present the study of structural and dynamical properties of form 0 using different complementary spectroscopic methods including powder X-ray diffraction, ^{1}H and ^{13}C solid state nuclear magnetic resonance (NMR), as well as quasielastic neutron scattering method (QENS). The quoted experimental results are discussed and interpreted in the light of density functional theory calculations. In particular we want to discern how the structure and crystal packing influence the dynamics of temazepam and to determine whether the crystallographic inequivalency of temazepam molecules causes differences in the dynamics of associated methyl groups. According to our best knowledge this is the first such broad study of temazepam.

II. EXPERIMENTAL AND COMPUTATIONAL DETAILS

Materials. Temazepam was purchased in a hermetically sealed container from Polfa Tarchomin S.A., Poznań. Its structure was controlled by PXRD, confirming the crystallographic structure reported in ref 7 (Form 0). The differential scanning calorimetry measurements, made in the range from 100 K to the melting point (431−433 K), have shown no phase transition in this temperature range.

Powder X-ray Diffraction. Powder X-ray diffraction studies of temazepam were carried out on a Empyrean (PANalytical) diffractometer using Cu Kα radiation (1.54 Å), reflection-transmission spinner (sample stage) and PIXcel 3D detector, operating in the Bragg−Brentano geometry. The 2 Theta scans were recorded at room temperature (300 K) in angles ranging from 5 to 60 (2Θ) with a step size of 0.013 (2Θ) and continuous scan mode.

Nuclear Magnetic Resonance (NMR) Studies. The powder sample for ^{1}H NMR studies was degassed and sealed off in glass ampules under vacuum. The measurement of the second moment of the proton NMR line was carried out as a function of temperature by a continuous wave spectrometer (constructed at the Radiospectroscopy Laboratory at the Faculty of Physics, AMU) operating on protons at the frequency of 28 MHz. ^{1}H NMR measurements of the spin−lattice relaxation time T_1 were performed using a Tecmag HF1 Apollo NMR console operating at 200 MHz and incorporating an Oxford Instruments magnet of 4.7 T. T_1 times were determined using the saturation−recovery sequence. The temperature of the sample was controlled in a dynamic Oxford helium flow cryostat and monitored by Oxford ITC 503 with the accuracy and stability of ±0.1 K.

^{13}C NMR spectra of temazepam were acquired using an Agilent spectrometer operating at Larmor frequency of 400 MHz for protons. The sample was placed within 4 mm diameter zirconia rotor and spun at 12 kHz frequency. The first 90° pulse applied to the proton channel was 5 μs long. The cross-polarization contact time was set to 850 μs. Two-pulse phase-modulated decoupling was utilized during the acquisition period. ^{13}C chemical shifts were referenced to the 38.3 ppm carbon signal of Adamantane, and 8k transients were accumulated.

Quasielastic Neutron Scattering. QENS measurements of temazepam were performed on the time-of-flight spectrometer IN6 and the backscattering spectrometer IN10 (ILL, Grenoble). The sample was placed in a flat aluminum sample holder of size 4 × 3 cm^2 and thickness of 0.15 mm (mass of the sample = 0.5 g). The mass and thickness of the samples were chosen to ensure that the transmission coefficient is between 0.85 and 0.90 and the multiple scattering contribution to the total scattering is less than 10%.

Measurements on IN6 were done at 300 and 150 K, using an incoming neutron wavelength equal to 5.12 Å and an energy resolution equal to 70 μeV (fwhm). The angle between the normal to the sample surface and the incident neutron beam was 135°.

Measurements on IN10 were performed at 100, 150, and 200 K with a better energy resolution (1 μeV (fwhm)). The incident wavelength was 6.27 Å and the angle between the normal to the sample surface and the incident neutron beam was 45°.

IN10 and IN6 data were corrected using the program LAMP,[9] which performs the standard corrections, including background subtraction, self-absorption geometric corrections, and self-shielding corrections. Then, using a vanadium spectrum as an elastic scattering standard, the intensities were normalized in order to correct for different detector efficiencies.

In the case of IN6, the detectors corresponding to wavevectors contaminated by Bragg reflections from the sample were removed from the data evaluation. In the case of IN10, as only 7 detectors that average over a large Q-range are available, this procedure is not possible.

Computational Details. Solid-state density functional theory (DFT)[10,11] computations were applied in order to understand the structural properties and magnetic response of the title system. The structure reported by Gałdecki[7] was used as the starting point in further geometry optimization. Periodic boundary conditions (PBC) calculations were carried out using a plane-wave pseudopotential method as implemented in CASTEP version 6.1.[12,13]

Although the substantial size of the system, including 12 molecules per unit cell, the computations were performed with high numerical accuracy. Exchange and correlation were defined using generalized gradient approximation (GGA) of rPBE functional as revised by Hammer[14] well as with the original PBE functional by Perdew.[15,16]

The computations were performed using designed nonlocal norm-conserving pseudopotentials (NC).[17] The plane wave kinetic energy cutoff of 1050 eV (77 Ry) was used along with the charge density grid multiplied by 3.5. Because of the studied system size, the electronic k-point sampling was limited to the Γ point.

The fixed-cell optimization was performed relaxing the fractional coordinates as well as optimizing only the hydrogen positions in the frame of the Gałdecki structure.[7] The optimization was performed with the convergence criteria for the total energy, maximum force, maximum atomic displacement, and SCF iterations smaller than 5×10^{-7} eV/atom, 0.0025 eV/Å, 5×10^{-5} Å, and 1×10^{-9} eV/atom, respectively. In order to examine the possible structural differences, induced by a selection of the exchange-correlation functional, the computations were also performed for several structures relaxed using different GGA approximations with the norm-conserving pseudopotentials. The results clearly confirmed the credibility of rPBE computations.

For the rPBE derived equilibrium structure, the phonon frequencies were obtained by diagonalization of dynamical matrices computed using density functional perturbation theory (DFPT),[18] confirming that the calculated structure is the equilibrium one. The phonon calculations are the topic of separate project; however, it should be mentioned that in order to keep the consistency, the computational methodology was

dx.doi.org/10.1021/jp502609b | J. Phys. Chem. B XXXX, XXX, XXX−XXX

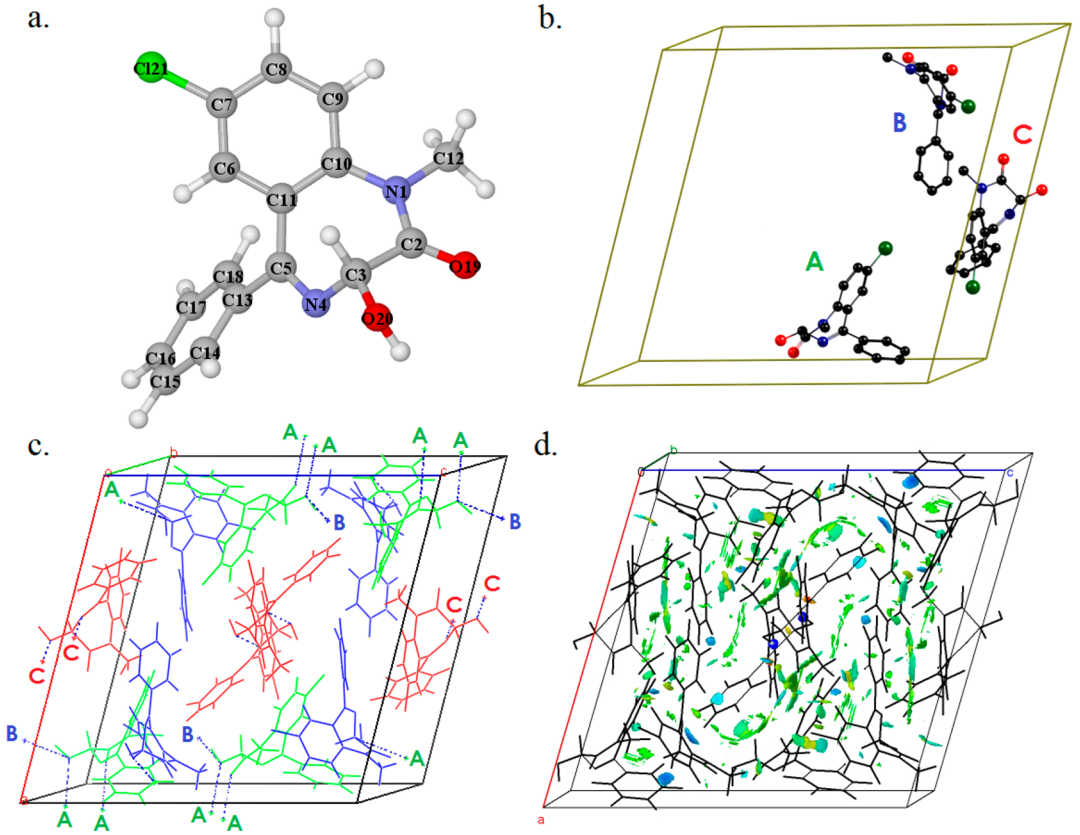

Figure 1. Structural view on temazepam. (a) The equilibrium geometries of a single molecule along with the adopted numbering system. (b) Asymmetric part of the unit cell with an applied notation of the nonequivalent molecules: A, B, C. (c) The unit-cell as optimized with plane-wave DFT rPBE/NC/1050 eV theory level, showing the symmetry equivalent molecules (A, green; B, navy; C, red). The net of hydrogen bonds presented as blue dotted lines. The hydrogen-bonded contact molecules beyond the cell are denoted with letters. (d) The corresponding noncovalent interactions (NCI) analysis isosurfaces as calculated from promolecular densities. The strong attractive interactions are colored in deep blue. Weak van der Waals forces are colored in blue, green, and yellow, following their repulsive character.

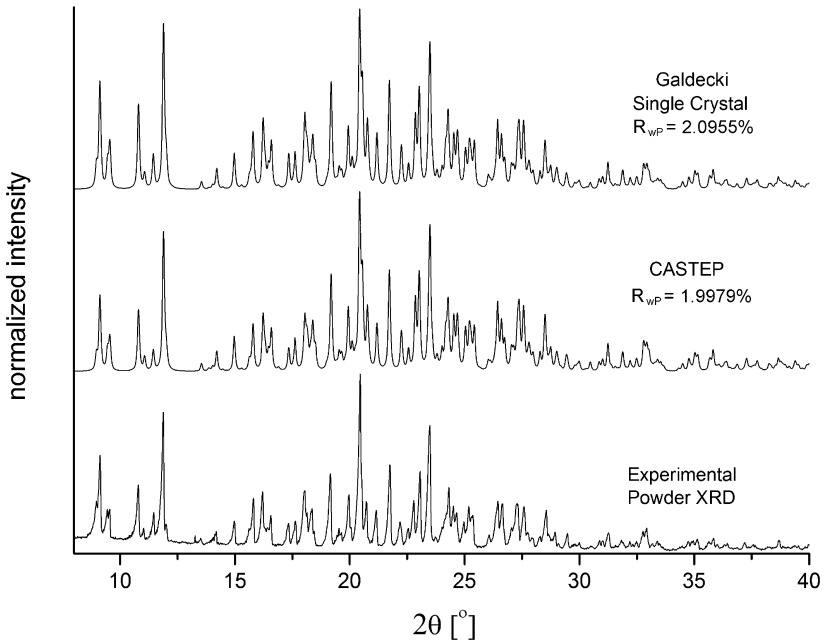

Figure 2. Experimental powder XRD spectrum of temazepam form 0 against the ones simulated from the structure reported by Galdecki[7] and plane-wave DFT at the rPBE/NC/1050 eV level of theory. The weighted-profile *R*-factors (R_{wF}) express the weighted sum of the squares of the difference between observed and calculated profile values.

dx.doi.org/10.1021/jp502609b | J. Phys. Chem. B XXXX, XXX, XXX−XXX

determined by the technical limitations of the actual linear-response implementation.

In order to estimate the theoretical reorientational barriers for the methyl groups reorientation, the constrained scans of the potential energy surfaces (rigid PES scan) were performed along the rotation of the methyl groups, keeping all the remaining coordinates fixed. In the case of such an extremely large system, further relaxation is unfortunately beyond the present computational resources. The rigid scans were performed for the equilibrium structures, using several models as quoted above. In order to estimate the reorientational barriers, the collective reorientations of the equivalent methyl groups were performed each 10°, calculating the electronic energy changes.

The NMR computations were performed with a gauge − including projected augmented-wave (GIPAW) method[19] as implemented in the NMR CASTEP module. The all-electron information, needed for calculation of the absolute NMR chemical shielding tensors, was finally reconstructed using on-the-fly ultrasoft pseudopotentials[20] at the plane-wave energy cutoff of 1050 eV (77 Ry) and SCF convergence tolerance of 1×10^{-13} eV/atom.

III. RESULTS

Structural Properties and Analysis of the Intermolecular Interactions. Chemically, temazepam (see Figure 1a−d) is a derivative of benzo-1,4-diazepine. The molecule of temazepam is built of a diazepinone ring, a seven-membered heterocyclic ring with nitrogen atoms at positions 1 and 4. As a result of condensation with a single benzene ring, the diazepinone ring forms a benzo-1,4-diazepine ring. The latter ring is substituted with a phenyl ring at C_5, a hydroxyl group at C_3 and at the first nitrogen atom it has a methyl group. The seven-membered diazepinone ring assumes a boat conformation with the hydroxyl group at the equatorial position. The possibility of hydrogen bond formation is a probable reason for different packing of molecules in the crystal.[7]

The crystal structure of temazepam (Form 0) was earlier described by Gałdecki.[7] The quoted polymorph crystallizes in the monoclinic system ($P21/c$ space group), containing three crystallographically independent molecules in the unit cell, denoted by convention[7] as A, B, and C, respectively (see Figure 1b,c). Recently, the possibility of obtaining 10 others polymorphic forms was described in ref 6. The authors solved the crystal structure of two anhydrous polymorphic forms of temazepam (called forms X and VI). These forms crystallize in *Pbca* and *P*-1 space groups, respectively, with two independent molecules per unit cell. It was also found that Form 0 is the thermodynamically most stable one.[6]

The plane-wave DFT structural relaxation was performed within the fixed unit-cell parameters reported by Gałdecki.[7] Figure 2 compares the powder diffraction spectra recorded for the measured sample along with the theoretical patterns, simulated both from the structure reported by Gałdecki[7] and from the CASTEP rPBE equilibrium model. An excellent agreement in both cases was found, which may be expressed by the weighted-profile *R*-factors (R_{wF}). The calculated global R_{wF} for the CASTEP related simulations (1.9979%) is even slightly better than for the structure reported by Gałdecki (2.0955%), confirming the high reliability of the theoretical geometry. An average disagreement between the theoretical and Gałdecki reported[7] non-hydrogen bond lengths may be expresed with following RMSD errors: r_{C-C} = 0.015 Å (*A* = 0.013 Å, *B* = 0.017 Å, *C* = 0.016 Å); r_{N-C} = 0.011 Å (*A* = 0.008 Å, *B* = 0.009 Å, *C* = 0.016 Å); r_{C-O} = 0.015 Å (A = 0.019 Å; B = 0.015 Å; C = 0.010 Å); r_{C-Cl} = 0.005 Å (A = 0.002 Å; B = 0.005 Å; C = 0.004 Å). It should be however mentioned that, as the authors claimed, the refinement of the structure was not straightforward.[7] The given hydrogen positions, taken from Fourier difference maps, are completely different from our computational results. The authors excluded the presence of hydrogen bonds in the system. In contrast, our computations clearly show the presence of three different nets of hydrogen bonding. In order to exclude the possible computational scenario, that hydrogen bonds may be created due to the significant conformational deformations of potentially flexible molecules, we have also performed the partial relaxation, keeping the non-hydrogen atoms fixed in the frame of data reported by Gałdecki.[7] The constrained optimization has confirmed that the studied structure is driven by the presence of hydrogen bonds, which are indeed easily formed without any conformational change.

In order to shed more light on the intermolecular interactions, the NCI analysis was applied.[21,22] NCI is a visualization index based on the electron density and its derivatives allowing for direct identification of the noncovalent interactions. In general, NCI is based on the analysis of the reduced density gradient (RDG) at low densities. Differentiation between the noncovalent interactions is based on the analysis of the sign of the second density Hessian eigenvalue times the density. This value is able to characterize the strength of the interaction by means of the density strength and its curvature.[21,22] However, the NCI representation is not only able to reveal the topological features of the density but also their effects in the 3D real space as well, by providing chemically intuitive isosurfaces. In Figure 1d, the NCI isosurfaces for the intermolecular interactions are plotted over the studied unit cell. The significantly attracting interactions (hydrogen-bondings) are visualized in deep blue. Weak van der Waals forces are colored in blue, green, and yellow, following their repulsive character. The analysis was performed using promolecular densities with the density cutoff = 0.3, using the NCI module implemented in JMOL ver. 12-2-0.[23]

The crystal analysis clearly shows that molecules C are bound into dimers, forming the net of N−H···O hydrogen bonds, toward the *b*-axis. Moreover, the molecules A join the adjacent unit cells in the *a*-axis direction, by the net of cyclic O−H···O bonds. The oxygen atoms in hydroxyl groups, linking the A molecules also share the hydrogen bonding with the neighboring OH groups from molecules B.

The crystal analysis also shows the long-range distribution of the stacking interactions between phenyl rings as the space is covered by weak attractive interactions. By analysis of the van der Waals forces, one may found that the ensemble of molecules C is in contact with molecules B via significant parallel stacking interactions between the phenyl rings. Simultaneously, the second phenyl rings from molecules C interact via T-shaped $\pi-\pi$ stackings with the adjacent phenyl rings in molecules B. Hence, it may be found, that molecules C and B are noticeably bounded by weak van der Waals forces.

By analysis of the CH_3 groups environment, we can find that methyl groups from molecules A and C are under the attractive potential of chlorine. It should be noted that methyls C are attracted by two chlorine atoms, associated with molecules A and B, while only single chlorine atom, associated with

dx.doi.org/10.1021/jp502609b | J. Phys. Chem. B XXXX, XXX, XXX−XXX

molecules B is in close contact with molecules A. Analysis of the bond lengths shows visible shortening of the N−C distance.

On the other hand, the methyl groups in molecules B feel the attractive potential of oxygens associated with molecules A. The oxygens are involved in the cyclic, resonance O−H···O hydrogen bonding, making the interactions character more complex. The N−C bond lengths analysis revealed nearly equivalent values for B and A molecules.

^{13}C NMR Solid State Study. The NMR chemical shift is strongly dependent on the molecular structure and on the inter- and intramolecular interactions that exist within a crystalline framework. The NMR studies were hence performed in order to shed more light on the subtle differences, linking the structural properties with intermolecular interactions.

However, in contrast to solvent NMR studies, the understanding of the solid state spectrum is much more difficult. The advantage of the GIPAW method, which was applied in our work, is that it enables the calculation of shielding parameters under periodic boundary conditions, thus implicitly accounting for intermolecular effects within the crystalline lattice. Another feature of the method is that it correctly accounts for the use of the pseudopotentials and the electronic core description in the calculations and therefore provides shielding constants with all-electron accuracy.[24]

The output of the first-principles NMR calculations is the absolute nuclear shielding tensor. In order to compare the results directly to experiment, one must convert the chemical shifts to the appropriate scale, what requires the shielding of the reference compound explicitly, which is often not the best choice. For ^{13}C (calibrated with respect to adamantane), the reference is tetramethylsilane (TMS), but full simulation of such liquid at room temperature would be a difficult task leading to additional errors, e.g., due to the ro-vibrational effects. The commonly acceptable procedure is hence to get the reference shielding from the intercept of the graph of calculated shieldings against the experimental shifts. The least-squares fit to a line of unit gradient, finally gives the value of 171 ppm, which was used as an effective reference for the presented computations.

Figure 3 presents the solid-state ^{13}C NMR spectra recorded experimentally against the ones computed with the GIPAW approach. We present the results obtained for both models, fully relaxed equilibrium structure and partially relaxed system with all the non-hydrogen atoms coordinates constrained according to Gałdecki.[7] As one may see, the fully relaxed structure stays in better overall agreement with the experiment. Hence all the chemical shifts were assigned according to the fully relaxed model and collected in Table 1.

The methyl groups associated with molecules B reveal different magnetic response from the others. In the NMR spectrum, CH_3 groups resonate at 35−37 ppm. The theory predicts the resonances at 32−35 ppm. The upper resonance found experimentally at 37 ppm may be assigned to the ensemble of molecules B, which were related to the hydrogen-bond close contacts. The lower resonances assigned to C and A molecules, which are in contact with chlorine atoms, are nearly degenerated, being predicted at ∼33 ppm. Such assignment is valid both for fully and partially relaxed models adapted here. It, however, does not simply reflects the N−C bond lengths hierarchy, found as B > A > C, where the bond lengths differences between A and B are of the order of 0.001 Å, which is in fact negligible and may be easily perturbed by the thermal motions.

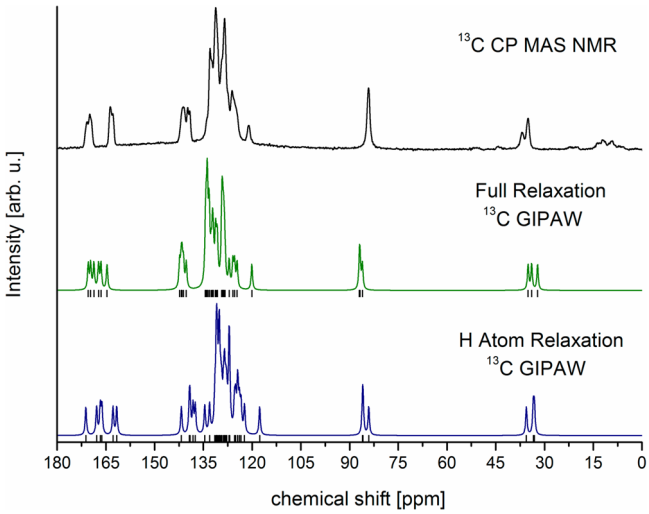

Figure 3. Experimental ^{13}C CP MAS NMR spectrum of temazepam along with the theoretical spectra calculated with the plane-wave DFT (rPBE/1050 eV) level of theory for both fully- and partially optimized structures.

The shortening of the C−O bond, associated with the hydroxyl groups, was observed in both models as following: B > A > C. Such effect seems to accompany the increasing hydrogen bond strength, as molecules C and A form cyclic hydrogen-bonded dimers and molecules B assist in the O−H···O bonding. However, the single resonance, recorded as a symmetric band at 84 ppm, may be assigned to the carbons associated with the hydroxyl groups. The theory predicts the resonances as nearly degenerated at ∼86 ppm. The more significant disagreement is found in the case of the partially optimized structure. The reason why the symmetric band related to the fully degenerated resonances is found in the experimental spectrum may be linked with the following factor. The thermal motions reveal that the hydrogen bond networks cannot be simply treated as a static system, especially since the theoretical computations are performed at 0 K while the experiment was performed at ambient conditions. The dynamic nature of the hydrogen bonded networks may hence result in averaging of the quoted resonances. The C═O related resonances are found as the highest ones, manifesting as a triplet in the experimental spectrum at ∼171, 170, and 169.5 ppm. The corresponding theoretical chemical shifts were found at ∼170.5, 170, and 169 ppm, respectively. Another triplet found at ∼164, 163.5, and 163 ppm is assigned to the carbon atoms linking the 1,4-benzodiazepine scaffold with the phenyl ring. These resonances were predicted by theory at ∼167, 166.5, and 164.5 ppm. The lower component may be assigned to the carbon atoms in molecules C forming the N−H···O bonding, while the remaining two are assigned to the molecules A and B with a similar character.

The set of resonances is found in the ^{13}C NMR spectrum at ∼140 ppm. Three upper resonances were found at 141.8, 141.2, and 140.9 ppm, combining into a broad band. These resonances were assigned to the carbon atom directly neighboring to the N−CH_3 part. Two another bands are found at 140.9 and 139.2 ppm along with a satellite band at 134 ppm. The resonances are assigned to the carbon atom linking the phenyl ring with the [1,4]-benzodiazepine scaffold. The significant downward shift of the carbon associated with molecules C indicates the influence of the N−H···O hydrogen

dx.doi.org/10.1021/jp502609b | J. Phys. Chem. B XXXX, XXX, XXX−XXX

Table 1. Collection of Experimental and Calculated ^{13}C NMR Isotropic Shifts for Temazepam[a]

		experimental			PBC-full relaxation		
^{13}C	fragment	A	B	C	A	B	C
C2	C═O	170.0	169.4	170.8	169.68	168.69	170.44
C3	C−OH	84.1	84.1	84.1	86.98	86.04	86.78
C5	B−DZ	163.7	163.3	162.9	167.26	166.51	164.65
C6	R_6^{DZ}	132.3	128.5	128.5	132.16	128.93	129.08
C7	R_6^{DZ}	134.0	133.0	132.3	134.40	133.93	131.92
C8	R_6^{DZ}	133.0	132.3	131.2	133.81	133.22	131.19
C9	R_6^{DZ}	124.5	125.0	121.1	124.63	125.41	120.09
C10	R_6^{DZ}	140.9	141.8	141.2	141.13	142.32	141.83
C11	R_6^{DZ}	131.2	133.0	130.5	130.66	133.78	129.24
C12	CH_3	35.1	36.9	35.1	32.14	35.05	33.96
C13	R_6^{B}	139.8	139.2	134.0	141.55	140.28	133.77
C14	R_6^{B}	132.3	133.0	132.3	133.33	134.23	133.18
C15	R_6^{B}	126.2	127.4	132.3	127.07	128.73	132.21
C16	R_6^{B}	131.2	127.4	132.3	130.84	128.36	132.63
C17	R_6^{B}	130.5	130.5	125.5	129.27	129.38	125.93
C18	R_6^{B}	133.0	127.4	131.3	134.18	128.61	131.31

[a]The theoretical data obtained using periodic DFT (PBC: CASTEP/rPBE/1050 eV) with fully relaxed coordinates (σ_{ref} = 171 ppm). The carbon numbering is consistent with Figure 1a. R_6, 6-membered ring; superscript DZ and B denote the [1,4]diazepine and 1H-benzo[*e*] parts, respectively.

bonding. The analysis of the phenyl ring orientation revealed that the <N−C−C−C torsional angle is much smaller in the case of the molecules C (22.6°) than for molecules A and B (39.9 and 35.4°, respectively). Significant influence of the intermolecular interactions on the related phenyl ring orientation has been revealed in the NCI analysis, where the conformation in molecules C is stabilized by the hydrogen bonding and stacking interactions with molecules A related phenyl rings.

The single resonance found at ∼121 ppm, along with the resonances contributing to the band at ∼125 ppm, is assigned to the neighboring carbon (denoted as C9). The shifted down, single resonance, is also assigned to molecules C.

Finally, very complex band covers the experimental spectrum in the range of ∼126−133 ppm. The band includes all the resonances related to remaining carbon atoms in the aromatic rings and cannot be simply distinguished.

Dynamics of Methyl Groups. To study molecular motions, especially dynamics of methyl groups in temazepam, two spectroscopic methods were applied, proton nuclear magnetic resonance (^1H NMR) and quasielastic neutron scattering (QENS). These two methods allow one to perform a detailed analysis of molecular reorientations in a wide temperature range.

The measurements of the second moment of the NMR line and spin−lattice relaxation time T_1 are shown in Figure 4. The value of M_2 (within the experimental error) does not change in the temperature range 100−370 K, and it is equal to about 6.6 G^2. Two minima of T_1 are observed at temperatures T = 133 and 83.3 K (1000/T = 7.5 and 1000/T = 12) and their values are equal to 1.3 and 2.2 s.

The temperature independence of the measured second moment may be due to two different reasons: (i) either no motion occurs in the temperature range studied (ii) or the observed plateau is the result of an average of the second moment by reorientation which starts below 100 K (i.e., below the lowest temperature available in our experiment). The existence of minima of relaxation time favors the second possibility. Taking into account the shape of the temazepam molecule is reasonable to assume the occurrence of

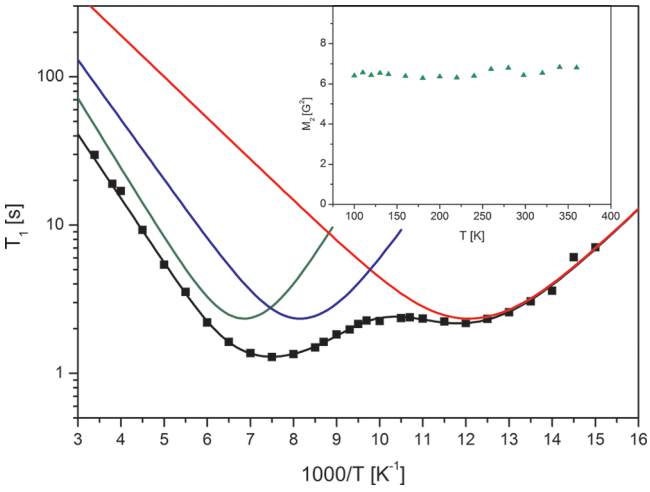

Figure 4. Relaxation time versus inverse temperature for temazepam at 200 MHz (■): the solid line (black) is the best fit according to eq 1 assuming three activation processes (green, blue, and red solid lines). Inset: second moment of NMR line versus temperature.

reorientation of a methyl group. Since the elementary unit cell contains three independent molecules of temazepam, it is also reasonable to consider the reorientation of three different methyl groups.

On the basis of crystallographic data[7] and using the van Vleck formula,[25] the second moment M_2 corresponding to the rigid lattice was calculated. Its value is equal to 12.3 G^2 and is much higher than the experimental value observed at the lowest temperature available experimentally. It is a hint for the measured M_2 that is averaged by molecular reorientations and that its frequency is greater than that corresponding to the line width for the rigid structure. As mentioned above, the most probable "candidates" for reorientation are methyl groups. Therefore, Monte Carlo simulations of second moment NMR lines[26] were performed with the assumption that all methyl groups can reorient. This kind of reorientation reduces the value of the second moment to 6.8 G^2, which is in very good agreement with the experimental value.

dx.doi.org/10.1021/jp502609b | J. Phys. Chem. B XXXX, XXX, XXX−XXX

On the basis of measurements of M_2, we could conclude that all methyl groups reorient, but this experiment did not allow one to tell more about their activation energy and/or correlation time. Such information was provided by measurements of the relaxation time. The well-known BPP formula was fitted to the temperature dependence of T_1:[27]

$$\frac{1}{T_1} = C\left[\frac{\tau_c}{1 + \omega_o^2\tau_c^2} + \frac{4\tau_c}{1 + 4\omega_o^2\tau_c^2}\right] \quad (1)$$

where $\tau_c = \tau_0 \exp(E_A/RT)$ is the correlation time (the Arrhenius relation), τ_0 is a constant, E_a is the activation energy, R is the gas constant, C is a relaxation constant, and ω_0 is the resonance frequency. To describe properly the temperature dependence of T_1, three activation processes are necessary (Figure 4) and the parameters obtained for the reorientation are summarized in Table 2, against the theoretical results

Table 2. Fit Activation Parameters and Relaxation Constant C Obtained for Temazepam by Fitting Equation 1 to Spin-Relaxation Experimental Points[a]

	experimental		
	1st process	2nd process	3rd process
E_a^{NMR} [kJ/mol]	9.0	7.7	5.3
τ_0 [s]	2.8×10^{-13}	2.5×10^{-13}	2.1×10^{-13}
C [1/s]	1.4×10^{9}	1.4×10^{9}	1.4×10^{9}
	theoretical activation barriers		
	molecule A	molecule B	molecule C
E_a^{rPBE} [kJ/mol]	12.7	10.6	6.5
$E_a^{rPBE\text{-}Exp}$ [kJ/mol]	12.4	9.5	5.3
$E_a^{PBE\text{-}TS}$ [kJ/mol]	13.0	8.8	6.1

[a]Theoretical activation barriers calculated with solid-state DFT in frame of full (E_a^{rPBE}, $E_a^{PBE\text{-}TS}$) and constrained relaxation ($E_a^{rPBE\text{-}Exp}$).

calculated using quoted models. The experimentally estimated activation barriers equal 9.0 ± 0.5, 7.7 ± 0.4, and 5.3 ± 0.2 kJ/mol, respectively. These values are comparable with those obtained for the reorientation of methyl groups in other compounds.[28−34]

The analysis has revealed three relaxation processes, which can be further linked with the reorientations of the methyl groups associated with three crystalographically inequivalent molecules A, B, and C, respectively. In order to assign the particular rotors, revealing different energy barriers, the rigid potential energy surface scans were performed for the selected models. The theoretical reorientation barriers were estimated for the models optimized in frame of full- (rPBE, PBE-TS) and constrained relaxation (rPBE-Exp). The PBE-TS equilibrium structure was obtained by including van der Waals corrections to the PBE functional, according to the Tkatchenko and Scheffler (PBE-TS) scheme.[35] The estimated reorientational barriers significantly differ for each methyl groups, confirming their dynamic inequivalency (see Table 2) and providing the unambiguous assignment as A, B, and C, respectively, following the lowering of the energy barriers. The assignment has been confirmed by all the applied models. Depending on the model, the energy barriers vary from 12.3 to 13.0 kJ/mol for methyl group A, 8.8−10.6 kJ/mol for molecules B, and 5.3−6.1 kJ/mol for molecules C. Although the calculated values are visibly higher than the experimental ones, their mutual energetic relations are comparable, delivering a good qualitative description of the studied system. However, the nature of the quantitative errors should be also noticed here. We believe that the most important error is due to the purely static nature of the computational methodology related to the absolute zero temperature, without including vibrational motions with an assumption of the system rigidity. We have performed the phonon computations, which provided the estimation of the methyl torsional modes energy. The calculated modes are spread over the range ∼100−225 cm^{-1}, that is 1.20−2.66 kJ/mol, in the following order C < B < A. The calculated lattice dynamics revealed that the maximally localized methyl torsions were observed at ∼160−165, ∼175−180, and 210−215 cm^{-1} for each methyl type. However, the low-wavenumber modes were found to be strongly coupled, which may affect the lowering of the reorientation barriers as the low-energy phonons can be easily thermally populated. The torsional methyl motions were found to be strongly delocalized as being significantly coupled to the deformation modes. Hence, we have observed that the methyl C torsional fluctuations are spread down to ∼100 cm^{-1}, combining with the phenyl ring torsions and phenyl out-of-plane deformations in molecules B. Such tendency may greatly affect the amount of polymorphism in the quoted system, as the molecular frame may be described as significantly flexible. We have found a significant coupling of methyl groups B and A, as the related torsional fluctuations are very likely mixed and most of the A and B torsional modes beneath 200 cm^{-1} are collective. Hence, the coupling may also affect the reorientation barrier, being another contribution to the discrepancy between the experimental and theoretical values. We believe that the dynamic nature of the crystal structure visibly lowers the rotational barriers affected by the crystal forces which tend to increase the barriers.

The biggest overestimation reaching 4 kJ/mol was found in the case of the first process, where the methyl groups A reorient under the potential of neighboring single chlorine atoms, associated with molecules B. However, the same groups reorient also in close-contact of the methyl groups associated with molecules B. The fluctuating distance beneath 3 Å may hence lead to the motion coupling, which could lower the experimental energy of both: methyls A and B. The smallest deviations were found with respect to the third process, related to methyls C, rotating under the potential of chlorine pairs in the similar equilibrium distance of ∼3.0−3.1 Å.

The next step of our study was the analysis of the quasielastic neutron scattering measurements performed on two spectrometers characterized by different resolution functions. The resolution and dynamical range of IN10 allows monitoring motions having characteristic times of the order of several hundreds of picoseconds or several nanoseconds, while IN6 allows to study faster motions.

Characteristic spectra of temazepam obtained on IN6 are shown in Figure 5. In all cases, the spectra were fitted with the following expression (convoluted with the resolution function $R(Q,\omega)$):

$$S(Q, \omega) = A_0(Q)\delta(\omega) + (1 - A_0(Q))L(\omega) + B(Q, \omega) \quad (2)$$

where $A_0(Q)$ is called the elastic incoherent structure factor, $L(\omega)$ is a Lorentz function of half-width Γ and $B(Q,\omega)$ describes the linear background. The spectra were fitted using the DAVE package,[36] which enables one to perform a numerical convolution with the instrumental resolution function $R(Q,\omega)$ determined from the vanadium measurement.

dx.doi.org/10.1021/jp502609b | J. Phys. Chem. B XXXX, XXX, XXX−XXX

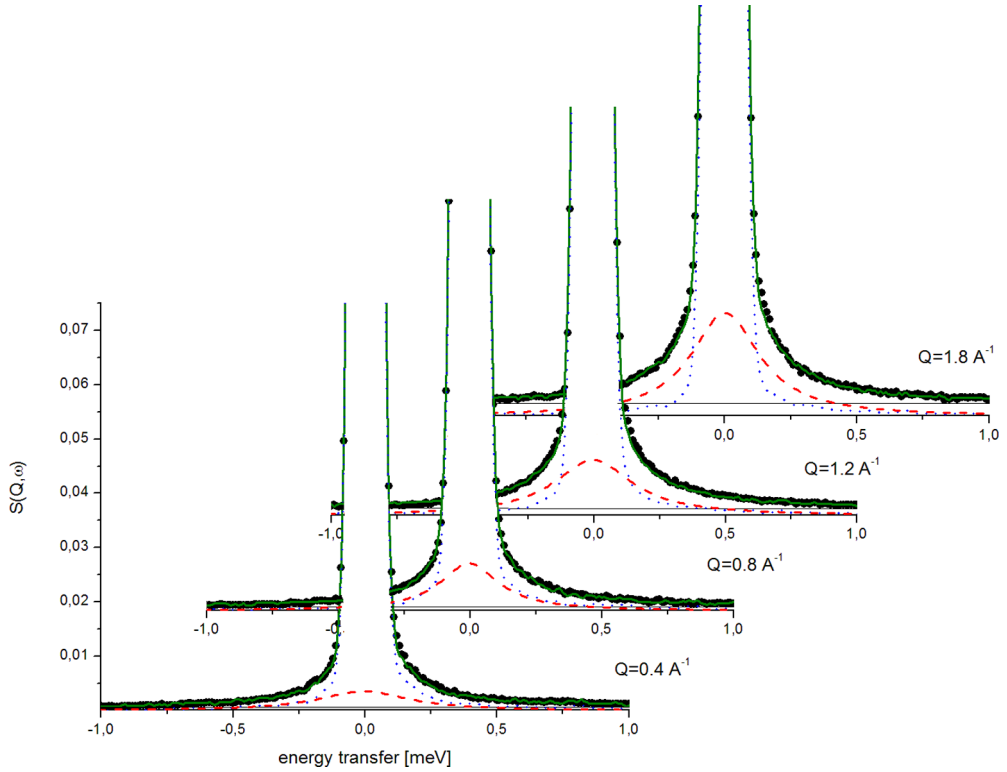

Figure 5. Normalized QENS spectra for temazepam measured on IN6 at 300 K for selected Q (points). The solid line (green) shows the fitted spectra, the dotted (blue) line corresponds to the resolution function, the dashed (red) line is the quasielastic contribution, and the dashed-dotted (black) lines are the background.

At all temperatures, a quasi-elastic broadening is clearly visible in both spectrometers and was well fitted using a single Lorentzian function. As we have three methyl groups that may reorient with different characteristic times we also performed additional fits assuming more than one Lorentzian function. However, the fits with a single Lorentzial very well reproduce the quasielastic broadening observed and we could not improve the fits using additional Lorentzians.

As the width of the Lorentzian function is reciprocal to the correlation time, this suggests two posibilities: either methyl groups have very similar correlation times and therefore appear as a single Lorentzian, or they may have very different correlation times such that only one group contributes to the quasielastic signal in the time-window of the spectrometer.

Two important parameters were extracted from the fitting: the correlation time (inversely proportional to the half-width of the Lorentz function Γ) and $A_0(Q)$, which provides information about the geometry of motion and is directly equal to the elastic incoherent structure factor (EISF). It means that this phenomenological fit permits us to determine the EISF in a model independent way.

Assuming jumps of methyl groups between three equidistance sites on a circle of radius r, the corresponding elastic incoherent structure factor can be written as[37]

$$A_0^{CH3}(Q) = \frac{1}{3}[1 + 2j_0(Qr\sqrt{3})] \quad (3)$$

While all atoms in the sample contribute to the EISF, the contribution from the hydrogen atoms represents more than 90% of the total scattering, so the contribution from other atoms (nitrogen, carbon, oxygen) can be neglected. It must be also noted that a fraction of the hydrogens can be immobile within the time scale corresponding to the spectrometer resolution and therefore we have

$$\mathrm{EISF}_{expt} = c + (1 - c)A_0^{CH3}(Q) \quad (4)$$

where the parameter c represents the ratio of immobile hydrogen atoms over the total number of protons (in three molecules of temazepam). The experimental elastic incoherent structure factor (EISF_{expt}, points) together with theoretical lines assuming that n = 1, 2, 3 methyl groups can reorient are displayed in Figure 6. At 150 K the experimental points are best described by the model of reorientations of only one methyl group, while at 300 K that the model where two methyl groups can reorient seems to hold.

The half-width Γ obtained from the fitting of the QENS spectra is related to the correlation time τ_c by $\Gamma = 3\hbar/(2\tau_c)$.[36] The temperature dependence of the correlation time established on the basis of NMR measurements (using the Arrhenius relation and activation parameters from Table 2) and τ_c from QENS experiment are displayed in Figure 7. The results obtained with both methods are in reasonable agreement with each other and allow one to follow the methyl groups dynamics as a function of temperature. The three methyl groups are dynamically inequivalent and characterized by different activation energies. At the lower temperatures, their correlation times are very different. Thus, at 100 K on IN10 and at 150 K on IN6 we observe the reorientation of one methyl group, associated with molecules C, with an activation energy of about 5 kJ/mol. Two other groups, namely, A and B, enter in the time-window of IN10 at 150 and 200 K and in the IN6 window at 300 K, and their correlation times are very similar.

dx.doi.org/10.1021/jp502609b | J. Phys. Chem. B XXXX, XXX, XXX−XXX

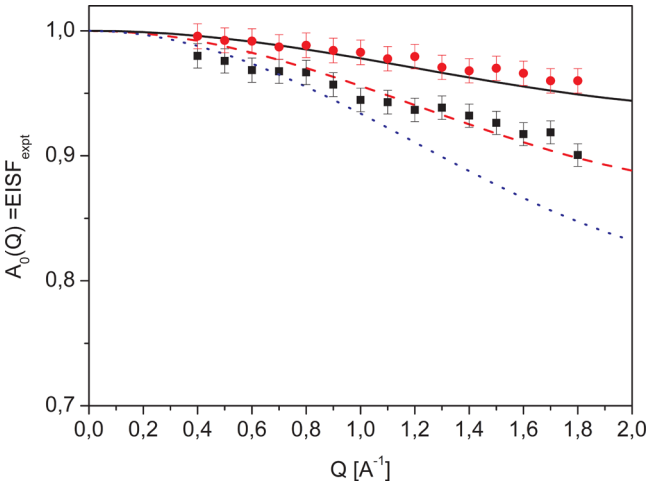

Figure 6. Experimental (red ● 150 K, ■ 300 K) elastic incoherent structure factor ($A_0(Q)$ = $EISF_{expt}$)) extracted from the fit to the spectra measured for temazepam on the IN6 spectrometer. Solid lines are the theoretical line obtained from eq 4 assuming reorientation of one (solid, black) two (dashed, red) or three (dotted, blue) methyl groups.

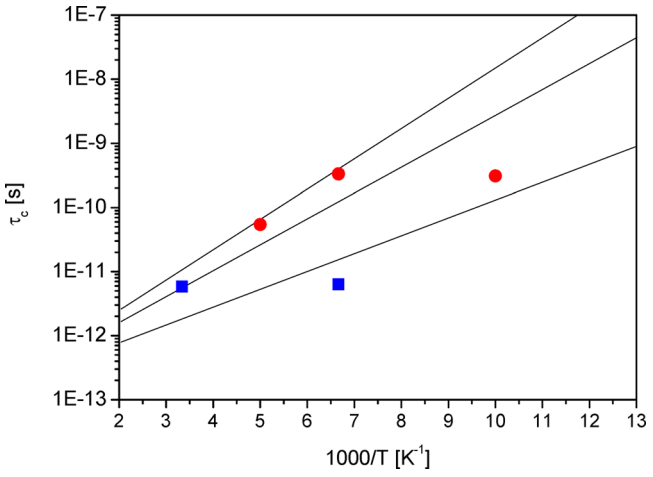

Figure 7. Correlation times obtained from QENS (blue ■) IN6, (red ●) IN10 and NMR measurements (solid lines). The error bars of τ_c extracted from QENS data have the size of the plotted symbols.

IV. CONCLUSIONS

The analysis of the structure of the equilibrium form of temazepam was refined by employing DFT calculations in periodic boundary conditions. The computations clearly revealed a significance of the intermolecular nets of hydrogen-bondings driving the phase structure, which were not previously reported. The extensive analysis focused on the nonequivalency of the asymmetric structural units and related methyl groups was proposed, by combining X-ray diffraction data with quantum-chemical calculations and intermolecular interactions analysis. The experimental studies linking QENS and spin−lattice relaxation ^{1}H NMR experiments provided clear insight into the methyl groups dynamics, delivering their activation parameters. Three processes were found and linked with the methyl groups associated with the crystallographically nonequivalent molecules. The reorientational barriers were estimated by periodic DFT calculations providing unambiguous assignment of the observed processes, which were further discussed in the frame of the related environment.

AUTHOR INFORMATION

Corresponding Author

*E-mail: aleksandra.pajzderska@amu.edu.pl. Phone: +48-61-829-5208. Fax: +48-61-829-5155.

Notes

The authors declare no competing financial interest.

ACKNOWLEDGMENTS

This research was supported in part by PL-Grid Infrastructure (Grant ID, postdoc). K. Drużbicki acknowledges the financial support of Polish Government Plenipotentiary for JINR in Dubna (Grant No. 118-8/1069-5/2014). Appreciation is also given to D. P. Kozlenko, D.Sc. (FLNP, JINR) for supporting the participation of K. Drużbicki in the CASTEP Training Workshop 2013. The work has been partially financed by the National Science Centre of Poland, Grant No. 2012/05/B/ST3/03176 and by the operating program POKL 4.1.1. Financial support from the National Centre for Research and Development under Research Grant "Nanomaterials and Their Application to Biomedicine", Contract Number PBS1/A9/13/2012, is also gratefully acknowledged.

REFERENCES

(1) Hasani, A.; Spiteri, M. A.; Pavia, D.; Lopez-Vidriero, M. T.; Agnew, J. E.; Clarke, S. W. Effect of Temazepam on Tracheobronchial Mucus Clearance. *Thorax* **1992**, *47*, 298−300.

(2) Welt, T.; Engelmann, M.; Renner, U.; Erhardt, A.; Muller, M. B.; Landgraf, R.; Holsboer, F.; Keck, M. E. Temazepam Triggers the Release of Vasopressin into the Rat Hypothalamic Paraventricular Nucleus: Novel Insight into Benzodiazepine Action on Hypothalamic-Pituitary-Adrenocortical System Activity During Stress. *Neuropsychopharmacology* **2006**, *31*, 2573−2579.

(3) Huang, Y.; Khoury, K.; Chanas, T.; Domling, A. Multicomponent Synthesis of Diverse 1,4-Benzodiazepine Scaffolds. *Org. Lett.* **2012**, *14*, 5916−5919.

(4) Hardtmann, G. E. Repic O. Vogt S. *Process for 3-hydroxy benzodiazepinones*. U.S. Patent 4,412,952, November 1, 1983.

(5) Reader E., Stempel A., Sternbach I. H. *Preparation of Certain Benzodiazepine Compounds*. U.S. Patent 3,340,253, September 5, 1967.

(6) Jetti, R. R; Karusala, N. R.; Singamsetty, R. K.; Gorantla, A. R.; Jonnalagadda, M.; Raval, C. K.; Namburu, L. R.; Datta, D.; *Novel polymorphic forms of temazepam and processes for preparing the same*. World Patent WO2010046929, April 29, 2010.

(7) Gałdecki, Z.; Główka, M. L. The Structure of a Psychoactive Agent: 7-chloro-3-hydroxy-1-methyl-5-phenyl-1,3-dihydro-2*H*-1,4-benzodiazepin-2-one (temazepam). *Acta Crystallogr.* **1980**, *36*, 3044−3048.

(8) Jetti, R. K. R.; Bhogala, B. R.; Gorantla, A. R.; Karusula, N. R.; Datta, D. Structural and Thermodynamis Features of Three Stable Crystal Dorms of Temazepam: A Sedative Drug. *Cryst. Growth Des.* **2011**, *11*, 2039−2044.

(9) http://www.ill.eu/instruments-support/computing-for-science/cs-software/all-software/lamp/.

(10) Hohenberg, P.; Kohn, W. Inhomogeneous Electron Gas. *Phys. Rev.* **1964**, *136*, B864−B871.

(11) Kohn, W.; Sham, L. J. Self-Consistent Equations Including Exchange and Correlation Effects. *Phys. Rev.* **1965**, *140*, A1133−A1138.

(12) Clark, S. J.; Segall, M. D.; Pickard, C. J.; Hasnip, P. J.; Probert, M. J.; Refson, K.; Payne, M. C. First Principles Methods Using CASTEP. *Z. Kristallogr.* **2005**, *220*, 567−570.

(13) Refson, K.; Clark, S. J.; Tulip, P. R. Variational Density-Functional Perturbation Theory for Dielectrics and Lattice Dynamics. *Phys. Rev. B* **2006**, *73*, 155114.
(14) Hammer, B.; Hansen, L. B.; Norskov, J. K. Improved Adsorption Energetics Within Density-Functional Theory Using Revised Perdew-Burke-Ernzerhof Functionals. *Phys. Rev. B* **1999**, *59*, 7413−7421.
(15) Perdew, J. P.; Burke, K.; Wang, Y. Generalized Gradient Approximation for the Exchange-Correlation Hole of a Many-Electron System. *Phys. Rev. B* **1996**, *54* (19), 16533−16539.
(16) Perdew, J. P.; Burke, K.; Ernzerhof, M. Generalized Gradient Approximation Made Simple. *Phys. Rev. Lett.* **1996**, *77*, 3865−3868.
(17) Rappe, A. M.; Rabe, K. M.; Kaxiras, E.; Joannopoulos, J. D. Optimized Pseudopotentials. *Phys. Rev. B* **1990**, *41*, 1227−1230.
(18) Refson, K.; Clark, S. J.; Tulip, P. R. Variational Density-Functional Perturbation Theory for Dielectrics and Lattice Dynamics. *Phys. Rev. B* **2006**, *73*, 155114.
(19) Pickard, C. J.; Mauri, F. All-electron Magnetic Response With Pseudopotentials: NMR Chemical Shifts. *Phys. Rev. B* **2001**, *63*, 245101.
(20) Yates, J. R.; Pickard, C. J.; Mauri, F. Calculation of NMR Chemical Shifts for Extended Systems Using Ultrasoft Pseudopotentials. *Phys. Rev. B* **2007**, *76*, 024401.
(21) Johnson, E. R.; Keinan, S.; Mori-Sánchez, P.; Contreras-García, J.; Cohen, A. J.; Yang, W. Revealing Noncovalent Interactions. *J. Am. Chem. Soc.* **2010**, *132*, 6498−6506.
(22) Contreras-García, J.; Johnson, E. R.; Keinan, S.; Chaudret, R.; Piquemal, J. P.; Beratan, D. N.; Yang, W. NCIPLOT: A Program for Plotting Noncovalent Interaction Regions. *J. Chem. Theor. Comp.* **2011**, *7*, 625−632.
(23) Hanson, R. M. Jmol - a Paradigm Shift in Crystallographic Visualization. *J. Appl. Crystallogr.* **2010**, *43*, 1250−1260.
(24) Yates, J. R.; Dobbins, S. E.; Pickard, C. J.; Mauri, F.; Ghi, P. Y.; Harris, R. K. A combined First Principles Computational and Solid-State NMR Study of a Molecular Crystal: flurbiprofen. *Phys. Chem. Chem. Phys.* **2005**, *7*, 1402−1407.
(25) Van Vleck, J. H. The Dipolar Broadening of Magnetic Resonance Lines in Crystals. *Phys. Rev.* **1948**, *74*, 1168−1183.
(26) Goc, R. Computer Calculation of The Van Vleck Second Moment For Materials With Internal Rotation of Spin Groups. *Comput. Phys. Commun.* **2004**, *162*, 102−112.
(27) Slichter, C. P. *Principles of Magnetic Resonance*, 3rd Enlarged and Updated ed.; Springer-Verlag: Berlin, Germany, 1996.
(28) Wasicki, J.; Kozlenko, D. P.; Pankov, S. E.; Bilski, P.; Pajzderska, A.; Hancock, B. C.; Medek, A.; Nawrocik, W.; Savenko, B. N. NMR Search for Polymorphic Phase Transformations in Chlorpropamide Form-A at High Pressures. *J. Pharm. Sci.* **2009**, *98*, 1426−1437.
(29) Mielcarek, J.; Nowak, D. M.; Pajzderska, A.; Peplinska, B.; Wasicki, J. A Hybrid Method for Estimation of Molecular Dynamics of Diazepam-Density Functional Theory Combined With NMR and FT-IR Spectroscopy. *Int. J. Pharm.* **2012**, *404*, 19−26.
(30) Pajzderska, A.; Chudoba, D. M.; Mielcarek, J.; Wąsicki, J. Calorimetric, FTIR and 1H NMR Measurements in Combination with DFT Calculations for Monitoring Solid-State Changes of Dynamics of Sibutramine Hydrochloride. *J. Pharm. Sci.* **2012**, *101*, 3799−810.
(31) Smuda, Ch.; Busch, S.; Schellenberg, R.; Unruh, T. Methyl Group Dynamics in Polycrystalline and Liquid Ubiquinone Q0 Studied by Neutron Scattering. *J. Phys. Chem. B* **2009**, *113*, 916−922.
(32) Smuda, Ch.; Gemmecker, G.; Unruh, T. Quasielastic and Inelastic Neutron Scattering Study of Methyl Group Rotation in Solid and Liquid Pentafluoroanisole and Pentafluorotoluene. *J. Chem. Phys.* **2008**, *128*, 194502−11.
(33) Colmenero, J.; Moreno, A. J.; Alegría, A. Neutron Scattering Investigations on Methyl Group Dynamics in Polymers. *Prog. Polym. Sci.* **2005**, *30*, 1147−1184.
(34) Prager, M.; Grimm, H.; Parker, S. F.; Lechner, R.; Desmedt, A.; McGrady, S.; Koglin, E. Methyl Group Rotation in Trimethylaluminium. *J. Phys.: Condens. Matter* **2002**, *14*, 1833−1845.
(35) Tkatchenko, A.; Scheffler, M. Accurate Molecular Van Der Waals Interactions from Ground-State Electron Density and Free-Atom Reference Data. *Phys. Rev. Lett.* **2009**, *102*, 073005.
(36) Azuah, R. T.; Kneller, L. R.; Qiu, Y.; Tregenna-Piggott, P. L. W.; Brown, C. M.; Copley, J. R. D.; Dimeo, R. M. DAVE: A Comprehensive Software Suite For The Reduction, Visualization, and Analysis of Low Energy Neutron Spectroscopic Data. *J. Res. Natl. Inst. Stand. Technol.* **2009**, *114*, 341−358.
(37) Bée, M. *Quasielastic Neutron Scattering: Principles and Applications in Solid State Chemistry, Biology, and Materials Science*; Adam Hilger: Bristol, England, 1988.